A Combined Experimental and Theoretical Study on the Stereodynamics of Monoaza[5]helicenes: Solvent-Induced Increase of the Enantiomerization Barrier in 1-Aza-[5]helicene

Tullio Caronna,*[a] Andrea Mele,*[b] Antonino Famulari,[b] Daniele Mendola,[b] Francesca Fontana,[a] Markus Juza,[c] Matthias Kamuf,[d] Kerstin Zawatzky,[d] and Oliver Trapp*[d]

Introduction

Pentahelicenes, hexahelicenes, and their higher homologues are chiral compounds forming helical structures of *ortho*-condensed aromatic rings with interesting, partially unexplored physicochemical properties, and potential applications spanning from optoelectronics to biological applications, catalysis, and chiral sensors.[1] Synthetic protocols were developed to obtain helicenes with skeletons consisting of *ortho*-fused benzene rings or analogue structures incorporating a heteroatom, as in thiophene-, furane-, or pyridine-containing helicenes.[2]

In recent years, a repertoire of synthetic strategies was developed to access all monoaza[5]helicenes as well as some diaza[5]helicenes.[3] By exploration of the unexpected broad range of physicochemical properties of aza[*n*]helicenes it was realized that there is an opportunity to modulate a specific property by controlled design of the position of the N atoms in the helical molecular frame. As paramount examples, we have already reported the dependence of the lifetime of the singlet and the triplet electronic states, ranging between 3.6 and 4.5 ns and 0.9 to 2.5 s, respectively,[4] as well as the half-life τ of racemization[5] ranging from 7 to 50 min depending on the position of the nitrogen atom.[6]

The preliminarily estimated interconversion barriers[5] and the importance to understand structural and electronic properties demands a detailed investigation of the stereodynamics of interconversion for the complete set of monoaza[5]helicenes **1**–**7** (Scheme 1) to be carried out both experimentally and by quantum chemical calculations. Theoretical calculations predict a considerably lower racemization barrier for monoaza[5]helicene **1** compared to monoaza[5]helicenes **2**–**7** and [5]helicene **8**.[7]

[a] *Prof. Dr. T. Caronna, Prof. Dr. F. Fontana*
Università di Bergamo, INSTM R.U. and Dipartimento di Ingegneria e Scienze Applicate Viale Marconi 5, 24044 Dalmine (Bergamo) (Italy)
E-mail: tullio.caronna@unibg.it

[b] *Prof. Dr. A. Mele, Prof. Dr. A. Famulari, Dr. D. Mendola*
Politecnico di Milano, Department of Chemistry Materials and Chemical Engineering "G. Natta"
Piazza L. da Vinci 32, 20132 Milano (Italy)
E-mail: andrea.mele@polimi.it

[c] *Dr. M. Juza*
Corden Pharma Switzerland LLC, Eichenweg 1, 4410 Liestal (Switzerland)

[d] *Dr. M. Kamuf, Dr. K. Zawatzky, Prof. Dr. O. Trapp*
Ruprecht-Karls Universität Heidelberg, Organisch-Chemisches Institut
Im Neuenheimer Feld 270, 69120 Heidelberg (Germany)
E-mail: trapp@oci.uni-heidelberg.de
Homepage: www.trapp.uni-hd.de

Results and Discussion

Enantioselective dynamic HPLC

The interconversion barriers of the complete set of monoaza[5]helicenes **1**–**7** and [5]helicene **8** (Scheme 1) were investigated. As already pointed out, enantiomerically pure samples of helicenes **1**–**8** show rapid racemization even at room temperature, therefore enantioselective dynamic HPLC (DHPLC)[8] in normal phase mode using *n*-hexane/2-propanol as the eluent was the method of choice for the precise determination of the enantiomerization[5] barriers. Excellent separations of the enantiomers of compounds **1**–**8** were achieved on coated and immobilized derivatized polysaccharide stationary phases[9] at temperatures below 10 °C.

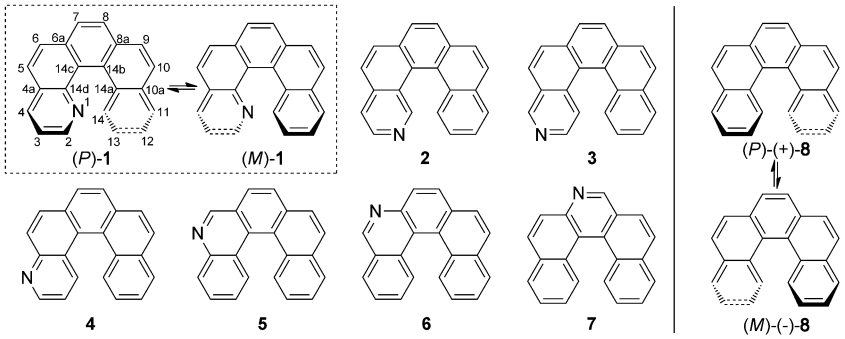

Scheme 1. Structures of the investigated monoaza[5]helicenes **1**–**7** and [5]helicene **8**. The interconversion between the (*P*)- and (*M*)-enantiomers of **1** and **8** is indicated by the equilibrium.

Surprisingly, a remarkably diverse set of separation conditions and chiral stationary phases were required for this family of monoaza[5]helicenes **1**–**7** (see the Supporting Information).

Temperature-dependent enantioselective DHPLC measurements were performed using UV and mass spectrometric detection in the single-ion monitoring (SIM) mode to avoid peak distortions by coeluting impurities with high absorption coefficients, commonly observed in helicenes. Representative elution profiles of the temperature-dependent chiral separation of 2-aza[5]helicene **2** and [5]helicene **8** are depicted in Figure 1. Distinct plateau formation caused by the dynamic enantiomerization of the monoaza[5]helicene at elevated temperatures and peak coalescence for temperatures above 55 °C were observed. For [5]helicene this behavior was shifted to significantly higher temperatures with hardly any interconversion at room temperature. Compared to its monoaza analogues, [5]helicene exhibits a preeminent stereointegrity. Reaction rate constants k and enantiomerization barriers $\Delta G^{\neq}$ were determined using the unified equation of dynamic chromatography[10] and an Eyring-plot analysis was performed for helicenes **1**–**8** to give activation parameters $\Delta H^{\neq}$ and $\Delta S^{\neq}$ from the temperature-dependent kinetic measurements. Figure 2 depicts the Eyring plots of [5]helicene **8** and 1-aza[5]helicene **1**, showing the high precision in the determination of the reaction rate constants.

The experimental activation parameters of the complete set of helicenes **1**–**8** are summarized in Table 1. These data extend previous experimental measurements of the racemization kinetics of carbohelicenes.[11] For comparison, the activation barrier $\Delta G^{\neq}$ obtained by DFT calculations (vide infra) and the differences between experimental and calculated values are also reported. [5]Helicene **8** shows as expected the highest Gibbs free activation energy $\Delta G^{\neq}$ (96.3 kJ mol^{-1} at 298 K). In general the enantiomerization barriers of aza[5]helicenes **1**–**7** are lower compared to the reference [5]helicene **8** irrespective of the position of the nitrogen atom in the molecular frame. The average value for the monoaza[5]helicenes is smaller by about 6 kJ mol^{-1}.

Additionally, differences can be found for the activation enthalpies $\Delta H^{\neq}$ between 41.7 and 63.5 kJ mol^{-1} and the activation entropies $\Delta S^{\neq}$ between −166 and −92 kJ mol^{-1}. Despite these variations in the activation parameters, the enantiomerization barriers $\Delta G^{\neq}$ are very similar. This can be explained by activation enthalpy/entropy compensations,[12,13] which typically depend on the chemical environment, for example, solvent influence and interaction with the (chiral) stationary phase.[8h] Here all measurements have been performed under comparable solvent compositions. The

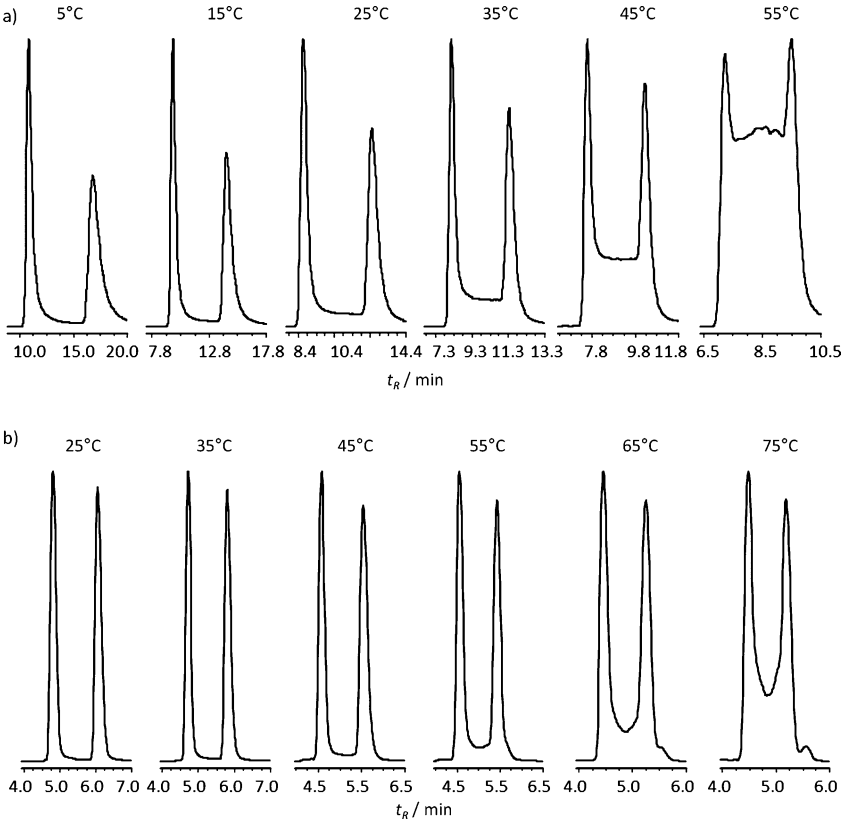

Figure 1. Selected chromatograms of a) 2-aza[5]helicene **2** and b) [5]helicene **8** at specified temperatures. For chromatographic conditions see the Supporting Information.

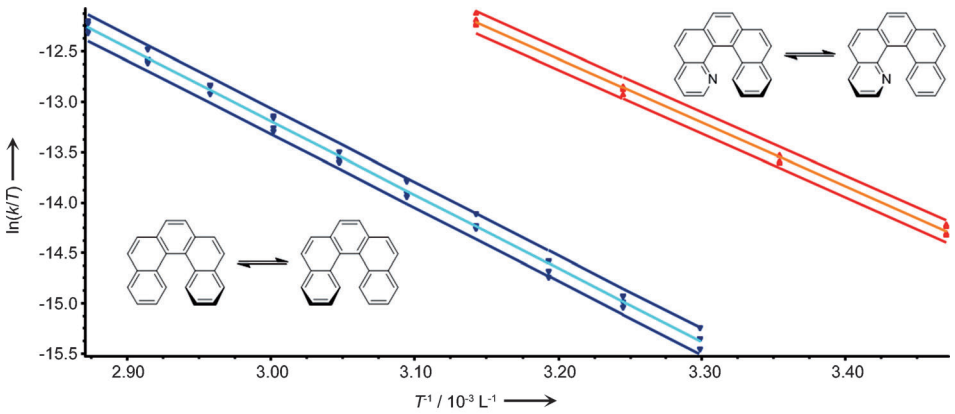

Figure 2. Eyring plot to determine activation parameters $\Delta H^{\neq}$ and $\Delta S^{\neq}$ of the enantiomerization barriers of [5]helicene **8** (left) and 1-aza-[5]helicene **1** (right).

Table 1. Activation parameters of the enantiomerization of aza[5]helicenes **1**–**7** and [5]helicene **8**. Chromatographic conditions are given in the Supporting Information.

Compd.	$\Delta G^{\neq}_{298K}$ [kJ mol^{-1}]	$\Delta H^{\neq}$ [kJ mol^{-1}]	$\Delta S^{\neq}_{298K}$ [J·(mol K)$^{-1}$]	$\Delta G^{\neq}_{298K}$[a] [kJ mol^{-1}]	$\Delta\Delta G^{\neq}_{298K}$[b] [kJ mol^{-1}]
1	90.7	52.9 ± 0.8	−127 ± 5	60.2	−30.5
2	90.9	63.5 ± 0.8	−92 ± 3	94.0	3.1
3	91.2	61.5 ± 1.5	−100 ± 5	95.2	4.0
4	92.3	44.9 ± 1.4	−159 ± 23	94.7	2.4
5	89.5	61.5 ± 0.8	−94 ± 3	91.2	1.7
6	91.2	41.7 ± 0.5	−166 ± 10	94.2	3.0
7	87.6	45.6 ± 0.9	−141 ± 8	88.5	0.9
8	96.3	60.8 ± 0.6	−119 ± 3	98.9	2.6

[a] DFT calculations at the B3LYP/6-311G(d,p) level of theory. [b] Difference between calculated and experimental Gibbs free activation energy.

values for the Gibbs free activation energy of compounds **2**–**8** obtained by DFT calculations are slightly higher, but in very good agreement with the measured values ($\Delta\Delta G^{\neq}$ 0.9–4.0 kJ mol^{-1}).

Quantum chemical calculations (DFT)

Surprisingly, 1-aza[5]helicene **1** shows a huge difference between the experimentally determined and calculated activation barrier. Therefore, in order to find a rational explanation for this deviation at the atomic level for the experimental data, we performed quantum chemical calculations at the B3LYP/6-311G(d,p) level to model the transition state of the enantiomerization. Recent dispersion-corrected (DFT-D) functionals are designed to provide an accurate description of van der Waals interactions.[14] The use of a long-range corrected hybrid functional with damped atom–atom dispersion, that is, ωB97X-D,[15] confirmed the reliability of the energies and geometrical parameters obtained at the B3LYP/6-311G(d,p) level. The ωB97X-D functional compares well with high-level coupled cluster calculations on relative stabilities of molecular conformations involving subtle, intramolecular C–H···π interactions.[16] The usage of dispersion correction revealed accurate results also in the case of solid state crystalline systems.[17] All calculations were performed using the GAMESS package.[18]

Modeling the transition-state (TS) of the enantiomerization process of [*n*]helicenes ($n = 3$–6 and 8) resulted in geometries passing through mirrored C_s molecular symmetries.[7] The structure of the TS and the corresponding enantiomerization barrier are influenced by the balance of repulsive interactions between terminal rings and the tendency to form planar conjugated aromatic structures. In the carbohelicene series, enantiomerization barriers are dependent on the number of *ortho*-condensed rings, substitution at various helix sites, and the modulation of steric hindrance on the terminal positions of the inner helix.[7] In the case of aza[5]helicenes, the presence and the position of the heteroatom may tune helicity parameters, such as dihedral angles and bond lengths, that modify the configurational stability and the enantiomerization barrier, thus affecting the potential applications in material science. Therefore the helicity parameters of compounds **1**–**8** were evaluated and compared by DFT calculations at the B3LYP/6-311G(d,p) and ωB97X-D/6-311G(d,p) levels. The calculations shed a light on the geometries and electronic structures as well as the enantiomerization pathway. Due to the presence of the heteroatom, transition-state and minimum structures are intrinsically of C_1 symmetry. The equilibrium or ground-state (GS) structures and the corresponding lowest barrier were calculated with only a single imaginary frequency (TS) in the gas phase without symmetry constraints. Solvent effects were not considered. Enantiomerization barriers $\Delta G^{\neq}$ were estimated as the difference of the total energy of the transition state (TS) and the equilibrium state (GS), both corrected for internal Gibbs free energy and zero-point vibrational energy. In all cases, the optimized transition state yielded a single imaginary frequency, confirming it as a saddle point. Analysis of the imaginary frequency shows that the saddle point is related to the vibration of the two terminal positions of the inner helix (atoms 1 and 14, see the Supporting Information, Figure QM1), which is consistent with the motion through the transition state.

The GS and TS structures of 1-aza[5]helicene, 2-aza[5]helicene, and 7-aza[5]helicene (compounds **1**, **2**, and **7** of Table 1) are reported in Figures QM3, QM4, and QM5 (see the Support-

ing Information). As already pointed out, the calculated $\Delta G^{\neq}_{298\,K}$ of **2**–**8** (Table 1) agree very well with the experimental values and the observed variation within the monoaza[5]helicenes. However, the activation barrier $\Delta G^{\neq}_{298\,K}$ obtained by DFT calculations of 1-aza[5]helicene (**1**) remarkably differs from all other aza[5]helicenes, as one would expect for the N atom at the 1-position of the polycondensed ring system due to the absence of transannular interactions C(1)–H···H–C(14) reducing the steric hindrance. Surprisingly, the experimental data show the opposite (vide infra). These calculations concerning compounds **1**, **2**, and **8** corroborate the findings recently published in an extensive study on pyrido[5]- and pyrido[6]helicene by Stary et al.[19] In particular, the calculated activation barriers $\Delta G^{\neq}_{298\,K}$ agree very well with the remarkably low barrier calculated for compound **1** and geometrical parameters are comparable, including the intramolecular improper blue-shifting hydrogen bond established in the TS of compound **1**.[16,20,21]

Some key structural parameters of the transition-state structures obtained by DFT calculations at the B3LYP/6-311G(d,p) level, describing the distortion of the fused rings system from planarity, are summarized in Table 2. The definition of the dihedral angles α, β, and γ is given in the footnotes of Table 2.

Table 2. Key structural parameters of transition-state structures obtained by DFT calculations on the B3LYP/6-311G(d,p) level of [5]helicene and aza[5]helicenes (see Scheme 1).

Compd.	X1-HC14 [Å]	α [°][a]	β [°][b]	γ [°][c]
1[d]	1.877[e]	−26.2	5.2	31.4
2	2.408	−38.0	−1.6	39.4
3	2.429	−39.5	−0.8	36.2
4	2.398	−37.0	−1.2	40.2
5	2.415	−36.8	0	37.1
6	2.366	−36.7	1.9	39.0
7	2.423	−36.6	−0.6	37.4
8	2.419	−38.8	0.0	38.8

[a] Dihedral angle between atoms 14-14a-14b-14c. [b] Dihedral angle between atoms 14a-14b-14c-14d. [c] Dihedral angle between atoms 14b-14c-14d-1. [d] For **1** the geometrical parameters were calculated at the ωB97X-D/6-311G(d,p) level in the order 1.867 Å, −29.9, 6.5, and 30.7°. The corresponding activation barrier $\Delta G^{\neq}$ is 59.0 kJ mol^{-1}. [e] See Scheme 1 for the assignment of the atoms C1-HC14 and N1-HC14, respectively.

All TS structures found for compounds **2**–**7** and [5]helicene **8** (Figures QM4 and QM5 in the Supporting Information) share the following geometrical features: $|\alpha| \approx |\gamma|$ and $\beta \approx 0$. The calculated values for α and γ span the range between −36.6 to −39.5 and 37.1 to 40.2°, respectively.

Additionally, C(1)–H···H–C(14) distances in the TS geometries of compounds **2**–**8** are significantly shorter than the sum of the van der Waals radii of the hydrogen and carbon atoms. The overall picture emerging from these data is that of a marked spatial distortion of the backbone of the conjugated π system. The associated lack of aromaticity, especially in the external six-membered ring, provides a significant contribution to the energy of the related transition states.

It is interesting to mention that compounds **5** and **7** show activation barriers lower than 90 kJ mol^{-1}, while all other values are higher. The calculated parameters of the corresponding TSs, especially γ and β, indicate that the torsion about the C(14a)–C(14b) and C(14b)–C(14c) bonds is less pronounced compared to the other aza-[5]helicenes, thus pointing out that the activation barriers are governed by small differences in the backbone structures.

The significant discrepancy between measured and calculated activation barrier $\Delta\Delta G^{\neq}_{298\,K}$ of 30.5 kJ mol^{-1} for compound **1** deserves attention. In 1-aza[5]helicene **1**, the N atom at the 1-position allows for a TS with a short contact distance N1–H(C14) of 1.8 Å, consistent with a weak but significant C–H···N interaction. The overall backbone geometry is less strongly deformed compared to that of **2**–**8** homologues (see α, β, and γ values in Table 2) resulting in a significant stabilization of the transition-state structure and thus explains the low enantiomerization barrier calculated for the gas-phase process.

As a model for understanding the unexpected difference between experimental DHPLC and calculated values in the gas phase for compound **1** (see Table 1), the influence of the presence of an explicit solvent molecule[22] was investigated. Hydrogen bonding and protonation were also considered in related studies to explain the dimerization and proton affinities of 1-aza[6]helicene and 2-aza[6]helicene determined by mass spectrometry.[23,24] The formation of a complex between **1** in its minimum-energy conformation GS and one 2-propanol molecule via an OH···N hydrogen bond (Figure 3) was simulated, resulting in an O(–H)···N distance of 2.95 Å (shorter than the sum of O and N van der Waals radii) and an O–H···N angle of about 150°. B3LYP/6-311G(d,p) and ωB97X-D/6-311G(d,p) calculations estimate intermolecular interaction energies of 28.5 and 29.0 kJ mol^{-1}, respectively, thus explaining the gap between the calculated and experimental energy barrier for compound 1. In fact, the formation of TS implies the disruption of this hydrogen bond because the nonbonding pair of the N atom oc-

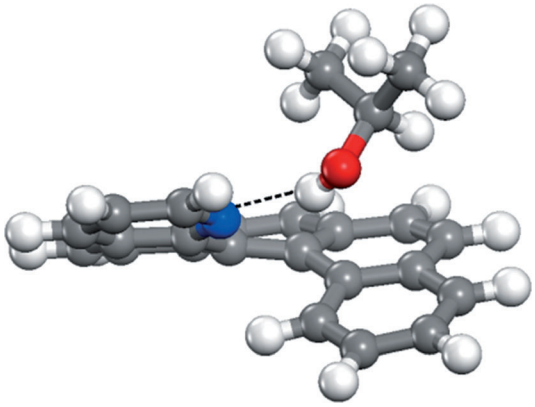

Figure 3. Calculated minimum-energy structure for the complex between monoaza[5]helicene **1** and one 2-propanol molecule via the OH···N hydrogen bond (N–O distance is 2.95 Å). Interaction energies of 28.5 and 29.0 kJ mol^{-1} calculated at the B3LYP/6-311G(d,p) and ωB97X-D/6-311G(d,p) levels, respectively.

cupies a sp^2-hybridized orbital strongly coordinated with the H–C(14) moiety. The nonbonding N pair becomes a poor hydrogen bond acceptor and it is no longer able to coordinate with isopropanol molecules thus accounting for the energy difference corresponding to the breakage of this hydrogen bond. Similar hydrogen bonds can be readily formed for compounds **2**–**7** through nitrogen atoms (see the Supporting Information, Figures QM6, QM7, and QM8) but in the latter cases the TS conformations could be reached without influencing these specific interactions.

Conclusion

In summary, we determined for the first time the activation parameters of [5]helicene and all seven monoaza analogs by enantioselective DHPLC. Formal substitution of a CH-group by a nitrogen atom in [5]helicene leads to significantly faster enantiomerization kinetics and therefore lower activation energies. Surprisingly, the position of the nitrogen atom has a significant influence on the activation parameters. DFT and DFT-D calculations of transition states allowed us to study, at the atomic level, the role played by the deviation of the whole ring system from planarity in driving the TSs' energy. Significant specific solute–solvent interactions were found to account for the unexpected difference in the TS energy of 1-aza[5]helicene **1** compared to the aza- and carbo-homologues (**2**–**8**), which triggers considerable conformational stability. Such an effect is highly interesting and might be exploited as a solvent sensor in optoelectronic applications, in which the electronic properties of 1-aza[5]helicene are modulated in presence of solvent molecules.

Acknowledgements

Generous financial support by the European Research Council (ERC) for a Starting Grant to OT (No. 258740, AMPCAT) is gratefully acknowledged. A.F. acknowledges CINECA for the computational resources.

[1] a) H. A. Staab, M. A. Zirnstein, C. Krieger, *Angew. Chem. Int. Ed. Engl.* **1989**, *28*, 86 – 88; *Angew. Chem.* **1989**, *101*, 73 – 75; b) H. Sugiura, D. Sakai, H. Otani, K. Teranishi, Y. Takahira, R. Amemiya, M. Yamaguchi, *Chem. Lett.* **2007**, *36*, 72 – 73; c) D. Nakano, M. Yamaguchi, *Tetrahedron Lett.* **2003**, *44*, 4969 – 4971; d) T. R. Kelly, *Acc. Chem. Res.* **2001**, *34*, 514 – 522; e) K. Tanaka, H. Osuga, Y. Kitahara, *J. Org. Chem.* **2002**, *67*, 1795 – 1801; f) T. J. Wigglesworth, D. Sud, T. B. Norsten, V. S. Lekhi, N. R. Branda, *J. Am. Chem. Soc.* **2005**, *127*, 7272 – 7273; g) L. Vyklický, S. H. Eichhorn, T. J. Katz, *Chem. Mater.* **2003**, *15*, 3594 – 3601; h) S. Sahasithiwat, T. Mophuang, I. Menbangpung, S. Kantonwong, T. Sooksimuang, *Synth. Met.* **2010**, *160*, 1148 – 1152; i) M. T. Reetz, E. W. Buettenmüller, R. Goddard, *Tetrahedron Lett.* **1997**, *38*, 3211 – 3214; j) M. T. Reetz, S. Sostmann, *J. Organomet. Chem.* **2000**, *603*, 105 – 109; k) M. T. Reetz, S. Sostmann, *Tetrahedron* **2001**, *57*, 2515 – 2520; l) M. Šámala, J. Míšeka, I. G. Stará, I. Starý, *Collect. Czech. Chem. Commun.* **2009**, *74*, 1151 – 1159; m) M. Gingras, *Chem. Soc. Rev.* **2013**, *42*, 1051 – 1095.

[2] Recent reviews of approaches to the synthesis of helicenes are: a) M. Gingras, *Chem. Soc. Rev.* **2013**, *42*, 968 – 1006; b) M. Gingras, G. Félix, R. Peresutti, *Chem. Soc. Rev.* **2013**, *42*, 1007 – 1050; c) Y. Shen, C.-F. Chen, *Chem. Rev.* **2012**, *112*, 1463 – 1535 and references cited therein.

[3] a) C. Bazzini, S. Brovelli, T. Caronna, C. Gambarotti, M. Giannone, P. Macchi, F. Meinardi, A. Mele, W. Panzeri, F. Recupero, A. Sironi, *Eur. J. Org. Chem.* **2005**, 1247 – 1257; b) S. Abbate, C. Bazzini, T. Caronna, F. Fontana, C. Gambarotti, F. Gangemi, G. Longhi, A. Mele, I. Natali Sora, W. Panzeri, *Tetrahedron* **2006**, *62*,139 – 148; c) T. Caronna, F. Fontana, A. Mele, I. Natali Sora, W. Panzeri, L. Viganò, *Synthesis* **2008**, 413 – 416; d) T. Caronna, S. Gabbiadini, A. Mele, F. Recupero, *Helv. Chim. Acta* **2002**, *85*, 1 – 8; e) T. Caronna, F. Castiglione, F. Fontana, D. Mendola, I. Natali Sora, *Molecules* **2012**, *17*, 463 – 479.

[4] K. Schmidt, S. Brovelli, V. Coropceanu, D. Beljonne, J. Cornil, C. Bazzini, T. Caronna, R. Tubino, F. Meinardi, Z. Shuai, J.-L. Bre′das, *J. Phys. Chem. A* **2007**, *111*, 10490 – 10499.

[5] M. Reist, B. Testa, P.-A. Carrupt, M. Jung, V. Schurig, *Chirality* **1995**, *7*, 396 – 400.

[6] S. Abbate, C. Bazzini, T. Caronna, F. Fontana, F. Gangemi, F. Lebon, G. Longhi, A. Mele, I. Natali Sora, *Inorg. Chim. Acta* **2007**, *360*, 908 – 912.

[7] a) R. H. Janke, G. Haufe, E.-U. Würthwein, J. H. Borkent, *J. Am. Chem. Soc.* **1996**, *118*, 6031 – 6035; b) S. Grimme, S. D. Peyerimhoff, *Chem. Phys.* **1996**, *204*, 411 – 417.

[8] a) J. Veciana, M. I. Crespo, *Angew. Chem. Int. Ed. Engl.* **1991**, *30*, 74 – 76; *Angew. Chem.* **1991**, *103*, 85 – 88; b) F. Gasparrini, L. Lunazzi, S. Alcaro, C. Villani, *J. Org. Chem.* **1995**, *60*, 5515 – 5519; c) I. D'Acquarica, F. Gasparri-ni, M. Pierini, C. Villani, G. Zappia, *J. Sep. Sci.* **2006**, *29*, 1508 – 1516; d) O. Trapp, V. Schurig, *J. Am. Chem. Soc.* **2000**, *122*, 1424 – 1430; e) O. Trapp, V. Schurig, *Comput. Chem.* **2001**, *25*, 187 – 195; f) O. Trapp, V. Schurig, *Chem. Eur. J.* **2001**, *7*, 1495 – 1502; g) O. Trapp, V. Schurig, *J. Chromatogr. A* **2001**, *911*, 167 – 175; h) F. Maier, O. Trapp, *Angew. Chem. Int. Ed.* **2012**, *51*, 2985 – 2988; *Angew. Chem.* **2012**, *124*, 3039 – 3043; i) F. Maier, O. Trapp, *Chirality* **2013**, *25*, 126 – 132.

[9] a) Y. Okamoto, E. Yashima, *Angew. Chem. Int. Ed.* **1998**, *37*, 1020 – 1043; *Angew. Chem.* **1998**, *110*, 1072 – 1095; b) E. Yashima, *J. Chromatogr. A* **2001**, *906*, 105 – 125; c) T. Ikai, C. Yamamoto, M. Kamigaito, Y. Okamoto, *Polym. J.* **2006**, *38*, 91 – 108; d) T. Zhang, P. Franco in *Chiral Separation Techniques*, (Ed. G. Subramanian) **2007**, Wiley-VCH, Weinheim, 3rd ed, pp. 99 – 134; e) T. Zhang, D. Nguyen, P. Franco, *J. Chromatogr. A* **2008**, *1191*, 214 – 222; f) L. Thunberg, J. Hashemi, S. Andresson, *J. Chromatogr. B* **2008**, *875*, 72 – 80; g) T. Zhang, P. Franco, D. Nguyen, R. Hamaski, S. Miyamoto, A. Ohnishi, T. Murakami, *J. Chromatogr. A* **2012**, *1269*, 178 – 188.

[10] a) O. Trapp, *Anal. Chem.* **2006**, *78*, 189 – 198; O. Trapp, *Chirality* **2006**, *18*, 489 – 497; b) O. Trapp, *Electrophoresis* **2006**, *27*, 2999 – 3006; c) O. Trapp, *Electrophoresis* **2007**, *28*, 691 – 696; d) O. Trapp, S. K. Weber, S. Bauch, W. Hofstadt, *Angew. Chem. Int. Ed.* **2007**, *46*, 7307 – 7310; *Angew. Chem.* **2007**, *119*, 7447 – 7451; e) O. Trapp, S. K. Weber, S. Bauch, T. Bäcker, W. Hofstadt, B. Spliethoff, *Chem. Eur. J.* **2008**, *14*, 4657 – 4666; f) O. Trapp, *Chemistry Today* **2008**, *26*, 26 – 28; g) O. Trapp, *J. Chromatogr. B* **2008**, *875*, 42 – 47; h) O. Trapp, S. Bremer, S. K. Weber, *Anal. Bioa-nal. Chem.* **2009**, *395*, 1673 – 1679; i) J. Troendlin, J. Rehbein, M. Hierse-mann, O. Trapp, *J. Am. Chem. Soc.* **2011**, *133*, 16444 – 16450.

[11] a) R. H. Martin, *Angew. Chem. Int. Ed. Engl.* **1974**, *13*, 649 – 660; *Angew. Chem.* **1974**, *86*, 727 – 738; b) C. Goedicke, H. Stegemeyer, *Tetrahedron Lett.* **1970**, *11*, 937 – 940.

[12] J. D. Dunitz, *Chem. Biol.* **1995**, *2*, 709 – 712.

[13] E. Grunwald, C. Steel, *J. Am. Chem. Soc.* **1995**, *117*, 5687 – 5692.

[14] a) S. Grimme, *J. Chem. Phys.* **2006**, *124*, 034108; b) J. Klimeš, A. Michae-lides, *J. Chem. Phys.* **2012**, *137*, 120901.

[15] a) J.-D. Chai, M. Head-Gordon, *Phys. Chem. Chem. Phys.* **2008**, *10*, 6615; b) J.-D. Chai, M. Head-Gordon, *J. Chem. Phys.* **2008**, *128*, 084106.

[16] a) A. Baggioli, S. V. Meille, G. Raos, R. Po, M. Brinkmann, A. Famulari, *Int. J. Quantum Chem.* **2013**, *113*, 2154 – 2162; b) A. Baggioli, A. Famulari, *Phys. Chem. Chem. Phys.* **2014**, *16*, 3983 – 3994.

[17] a) F. Guo, M.-Q. Zhang, A. Famulari, J. Martí-Rujas, *J. CrystEngComm* **2013**, *15*, 6237; b) H. Y. Guan, Z. Wang, A. Famulari, X. Wang, F. Guo, J. Martí-Rujas, *J. Inorg. Chem.* **2014**, *53*, 7438 – 7445; c) F. Guo, H. D. Shao, Q. Yang, A. Famulari, J. Martí-Rujas, *J. CrystEngComm* **2014**, *16*, 969 – 973.

[18] a) M. W. Schmidt, K. K. Baldridge, J. A. Boatz, J. S. T. Elbert, M. S. Gordon, J. H. Jensen, S. Koseki, N. Matsunaga, K. A. Nguyen, S. Su, T. L. Windus, M. Dupuis, J. A. Montgomery, *J. Comput. Chem.* **1993**, *14*, 1347; b) M. S. Gordon, M. W. Schmidt in *Theory and Applications of Computational Chemistry, The First Forty Years* (Eds.: C. E. Dykstra, G. Frenking, K. S. Kim, G. E. Scuseria), Elsevier, Amsterdam, **2005**, pp. 1167 – 1189.
[19] J. V. Chocholousova, J. Vacek, A. Andronova, J. Misek, O. Songis, M. Samal, I. G. Stara, M. Meyer, M. Bourdillon, L. Pospisil, I. Stary, *Chem. Eur. J.* **2014**, *20*, 877 – 893.
[20] P. Hobza, Z. Havlas, *Chem. Rev.* **2000**, *100*, 4253 – 4264.
[21] A. Famulari, G. Raos, A. Baggioli, M. Casalegno, R. Po, S. V. Meille, *J. Phys. Chem. B* **2012**, *116*, 14504 – 14509.
[22] 2-Propanol was selected due to its presence as a polar solvent component in all experiments.
[23] J. Roithová, D. Schröder, J. Misek, I. G. Stara, I. Stary, *J. Mass Spectrom.* **2007**, *42*, 1233 – 1237.
[24] J. Mísek, M. Tichy, I. G. Stará, I. Stary, J. Roithová, D. Schröder, *Croat. Chem. Acta* **2009**, *82*, 79 – 86.